5th SASTech Iran | Mashhad May 12 - 17 | 2011
5th Symposium on Advances in Science & Technology

Modeling of Sediment Transport Conditions due to Dam-break

SALEH AMIN YAVARI[1, 2]
[1]Islamic Azad University of CHALOOS, civil engineering group, opposite of Imam Hussein mosque, 17 Shahrivar Avenue, CHALOOS, MAZANDERAN
And
[2] MODERN SAZEH TONKA Co.
Email: saleh1161a@gmail.com

Paper Reference Number: 1611-118
Name of the Presenter: SALEH AMIN YAVARI

Numerical simulation of sediment transport has been conducted in two modes, namely one-layer and two-layer modelling. In one-layer approach, water surface and bed elevation variations due to dambreak have been modelled and in the two-layer approach, a second layer combining water and sediment has been added. Finite volume techniques, HLL, have been utilised for discretization of the relationships and a GIS tool has been added for enhancement of interpretations of the simulation results. Application of the one-layer model showed a good agreement in simulation of the wave front, shock waves and discontinuities. In the case of the two-layer model, sediment transport was shown to be the result of differences in the shear stresses in bed material, the sediment, the bed profile and water surface profile were accurately simulated. In comparison with experimental results, it has been shown that larger shear stresses in the bed than the sediment would result in sedimentation and inversely would result in erosion. Discontinuities and shock waves were accurately modelled. The model developed may be used to estimate the amount of sediment produced as a result of dambreak.
Keywords: Sediment transport, Dambreak, GIS, Numerical simulation

1. Introduction

Dam-break floods can significantly rework the morphology of erodible valleys. Within laterally constrained channels, dam-break induced erosion has been analysed by Capart & Young (1998) and Fraccarollo & Capart (2002). In the near field, rapid and intense erosion accompanies the development of the dambreak wave. The flow exhibits strong free surface features: wave breaking occurs at the center (near the location of the dam), and a nearly vertical wall of water and debris overruns the sediment bed at the wave forefront (Capart, 2000), resulting in an intense transient debris flow. To account for inertia while still adopting simple assumptions, Capart (2000) has proposed to tackle the problem by using an extended shallow-water description: the flow is divided in three separate layers, namely a pure-water layer, a transport layer of finite thickness formed by a mixture of water and sediments, and a motionless sediment substrate. The layers are divided by sharp interfaces and the erosion of the sediment bed is displayed as a phase change of the bed material, undergoing a transition from solid-like to fluid-like behavior as it is entrained by the flow. The dam-break wave and the associated erosion and deposition feature can be two- and three-dimensional patterns; for example the velocity at the early stage of the wave has a significant vertical component. This

is also the case for pure hydrodynamic flow; however it will be shown that depth-averaged models give valuable results, with significantly less computational effort than 3D models. In the present case, the improvement of one-dimensional models revealed to be fruitful, yielding surprisingly accurate results.

2. Research Methodology

2.1 Dam break problem

A problem of considerable physical interest is the so-called dam-break problem. Assume a horizontal channel of uniform, rectangular cross section. Suppose furthermore that the channel has two uniform water levels, both at rest, separated by a wall at position x=0. If wall separating the two uniform levels of water collapse, two dominate feature will emerge from the process in the form waves. A right facing wave travels into the shallow situation of fluid, increasing the depth abruptly. The left facing wave travels into deep water region and has the effect of reducing on the free surface height. The wave pattern emerging is almost that is centered wave system with a left refraction wave and a right shock wave; such wave systems may be approximated by the shallow water equation. (Fig. 1)

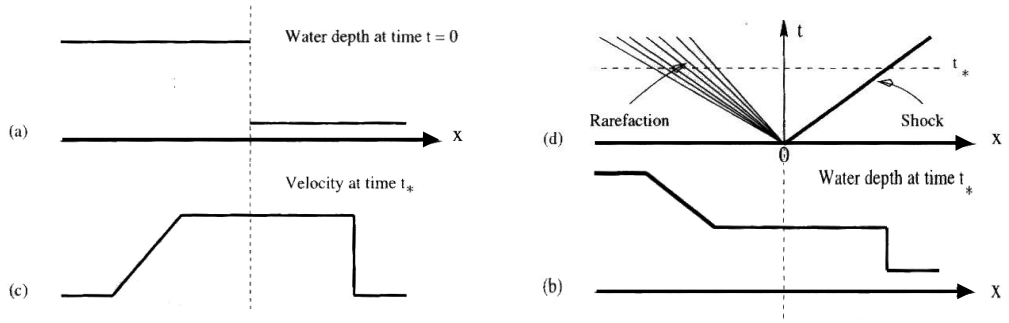

Fig 1: time evolution of the dam break problem (a) initial depth (b) depth at a later time and (c) corresponding velocity distribution; (d) wave diagram of the full process on the x-t plane.

2.2 Riemann problem

The Riemann problem of the shallow water equation is a generalization of the dam break problem. Formally, the Riemann problem is defined as the initial value problem (IVP)

$$U_t + F(U)_x = 0\,, \qquad U(x,0) = \begin{cases} U_L & \text{if } x < 0 \\ U_R & \text{if } x > 0 \end{cases}, U_L = \begin{bmatrix} h_L \\ h_L u_L \\ h_L v_L \end{bmatrix}\,,\; U_R = \begin{bmatrix} h_R \\ h_R u_R \\ h_R v_R \end{bmatrix} \quad (1)$$

We have two distinct classes of methods for solving Riemann problem, Godunov-type methods or upwind methods and centered methods. For shallow water equation there is not a very strong case for utilizing centered methods, as the equations are indeed very simple.

The upwind method of Godunov is a numerical scheme, the main feature of which is that it utilizes the solution of the Riemann problem locally; this solution can be exact or approximate. Making the choice between the exact and approximate Riemann solvers is motivated by (i) computational cost (ii) simplicity and (iii) correctness, which in this paper was used approximate solution.

The updating conservative formula for (Eq.1) is

$$U_i^{n+1} = U_i^n - \frac{\Delta t}{\Delta x}\left[F_{i+\frac{1}{2}} - F_{i-\frac{1}{2}}\right] \quad (2)$$

There are several approximate –state Riemann solvers. The HLL Riemann solver of Harten, Lax and van Leer, HLLC modification of Toro et al, HLLE of Davis and Einfelt, LHLL of Fraccarollo et al, approximate Riemann solver of Roe and the Riemann solver of Osher and Solomon. In this paper were used HLL, HLLC and LHLL methods for solution partial differential equations (PDEs). In this paper, the HLL, HLLC and LHLL methods have been used to solve the partial differential equations (PDEs).

2.3. The HLL solver

Harten, Lax and van Leer suggested a way of solving the Riemann problem approximately by finding directly an approximation to the numerical flux $F_{i+\frac{1}{2}}$. The HLL approach estimates S_L and S_R for the smallest and largest signal velocities in the solution Riemann problem with data $U_L = U_i^n$, $U_R = U_{i+1}^n$ and corresponding fluxes $F_L = F(U_L)$, $F_R = F(U_R)$.
One derives the HLL numerical flux as

$$F_{i+\frac{1}{2}} = \begin{cases} F_L & \text{if} \quad S_L \geq 0 \\ F^{HLL} = \frac{S_R F_L - S_L F_R + S_R S_L (U_R - U_L)}{S_R - S_L} & \text{if} \quad S_L \leq 0 \leq S_R \\ F_R & \text{if} \quad S_R \leq 0 \end{cases} \tag{3}$$

$$S_R = u_R + q_R\sqrt{gh_R} \qquad S_L = u_L - q_L\sqrt{gh_L} \tag{4}$$

Where q_k (K=L, R) is given by

$$q_K = \begin{cases} \sqrt{\frac{1}{2}\frac{(h_* + h_K)h_*}{{h_K}^2}} & \text{if} \quad h_* > h_K \\ 1 & \text{if} \quad h_* \leq h_K \end{cases} \tag{5}$$

$$h_* = \frac{1}{2}(h_L + h_R) - \frac{1}{4}(u_R - u_L)(h_L + h_R)/(a_L + a_R) \tag{6}$$

For the augmented system allowing for shear waves or species equations, the HLL approach is founded to be inadequate, as it ignores the middle wave.

2.4 The HLLC solver

The HLLC approximate Riemann solver is modification of the basic HLL scheme to account for the influence of intermediate waves.

$$F_{i+\frac{1}{2}}^{HLLC} = \begin{cases} F_L & \text{if} \quad S_L \geq 0 \\ F_{*L} & \text{if} \quad S_L \leq 0 \leq S_* \\ F_{*R} & \text{if} \quad S_* \leq 0 \leq S_R \\ F_R & \text{if} \quad S_R \leq 0 \end{cases} \tag{7}$$

$$F_{*L} = F_L + S_L(U_{*L} - U_L) \quad , \quad F_{*R} = F_R + S_R(U_{*R} - U_R) \tag{8}$$

The states U_{*L} , U_{*R} are given by

$$U_{*K} = h_K\left(\frac{S_K - U_K}{S_K - S_*}\right)\begin{bmatrix} 1 \\ S_* \\ \varphi_K \end{bmatrix} \tag{9}$$

$$S_* = \frac{1}{2}(u_L + u_R) - (h_R - h_L)(a_L + a_R)/(h_L + h_R) \tag{10}$$

2.5 The LHLL solver

A Godunov-type method is based on the HLL Riemann-solver. The main innovation in LHLL is in the treatment of the nonconservative flux, which is managed in partially unsplitted way. It has been successfully applied to the benchmark case of the erosional dam-break flood over an initial horizontal-bed.

$$F_{L,R}^{LHLL} = F^{HLL} - \frac{S_{L,R}}{S_L - S_R} g\tilde{h}\left(z_b^R - z_b^L\right),\ \tilde{h} = 0.5(h_R + h_L)$$
$$S_L = \min\left(\lambda_{1,L}, \lambda_{1,R}\right) \quad ,\ S_R = \max\left(\lambda_{3,L}, \lambda_{3,R}\right) \tag{11}$$

Being $\lambda_{1,L,R}$, $\lambda_{3,L,R}$ respectively, the minimum and maximum local eigenvalues associated to the one-dimensional version of system and evaluated with the values of the variables at the right side and left side of the discontinuity.

Two types of one-dimensional models are presented in this paper: (1) the common Saint-Venant–Exner approach generally used for describing the long-term geomorphic evolution in rivers; (2) the basic two-layer model proposed by Capart (2000) where the velocities of water and sediment layers are considered as unique.

2.6 One-layer description

Most of the available models describing the geomorphic evolution of movable-bed rivers in presence of transient flow rely on Saint-Venant continuity and momentum equations:

$$\frac{\partial h}{\partial t} + \frac{\partial q}{\partial x} == 0$$
$$\frac{\partial q}{\partial t} + \frac{\partial}{\partial x}\left(\frac{q^2}{h}\right) + gh\frac{\partial h}{\partial x} = gh(S_0 - S_f) \tag{12}$$
$$\frac{\partial Z_b}{\partial t} + \frac{1}{1-\varepsilon_0}\frac{\partial q_s}{\partial x} = 0$$

Estimation of the sediment transport capacity using the empirical formula Meyer-Peter–Müller

$$q_s(q,h) = 8\sqrt{g(s-1)d_{50}^3}\left(\frac{n^2q^2}{(s-1)d_{50}h^{\frac{7}{3}}} - 0.047\right)^{\frac{3}{2}} \tag{13}$$

According to the section 2.2

$$\frac{\partial U}{\partial t} + \frac{\partial F(U)}{\partial x} + H(U)\frac{\partial U}{\partial x} = S(U)$$
$$U = \begin{pmatrix} h \\ q \\ z_b \end{pmatrix} \ ,\ F(U) = \begin{pmatrix} q \\ \frac{q^2}{h} + g\frac{h^2}{2} \\ \frac{q_s}{1-\varepsilon_0} \end{pmatrix} = \begin{pmatrix} q \\ \sigma \\ \psi \end{pmatrix} \ ,\ H(U) = \begin{pmatrix} 0 & 0 & 0 \\ 0 & 0 & gh \\ 0 & 0 & 0 \end{pmatrix},\quad S(U) = \begin{pmatrix} 0 \\ -ghS_f \\ 0 \end{pmatrix} \tag{14}$$

This PDE have three eigenvalues

$$a_1 = \frac{2q}{h} \ ,\ a_2 = \frac{q^2}{h^2} - gh - \frac{gh}{1-\varepsilon_0}\frac{\partial q_s}{\partial q} \quad ,\quad a_3 = \frac{gh}{1-\varepsilon_0}\frac{\partial q_s}{\partial h} \tag{15}$$

By using finite volume method (FVM), the integral form (Eq. 14) of the conservation laws become

$$U_i^{n+1} = U_i^n - \frac{\Delta t}{\Delta x}\left[\left(F_{i+\frac{1}{2}}^* + H_i U_{i+\frac{1}{2}}^*\right) - \left(F_{i-\frac{1}{2}}^* + H_i U_{i-\frac{1}{2}}^*\right)\right] + S_i^n \Delta t \tag{16}$$

The integral form water continuity equation (Eq.12) becomes

$$h_i^{n+1} = h_i^n - \frac{\Delta t}{\Delta x}\left(q_{i+\frac{1}{2}}^* - q_{i-\frac{1}{2}}^*\right) \tag{17}$$

Fluxes $q_{i+\frac{1}{2}}^*, q_{i-\frac{1}{2}}^*$ were estimated by the HLL Riemann solver because this equation has no source term (intermediate wave). Integral form momentum water equation (Eq.12) becomes

$$q_i^{n+1} = q_i^n - \frac{\Delta t}{\Delta x}\left[\sigma_{i+\frac{1}{2}}^* + gh_i Z_{b,i+\frac{1}{2}}^* - \sigma_{i-\frac{1}{2}}^* - gh_i Z_{b,i-\frac{1}{2}}^*\right] - (ghS_f)_i^n \Delta t \tag{18}$$

For solving fluxes $\sigma^*_{i+\frac{1}{2}}, \sigma^*_{i-\frac{1}{2}}$ and $Z^*_{b,i+\frac{1}{2}}, Z^*_{b,i-\frac{1}{2}}$ HLL method LHLL solver were employed, respectively

$$q_i^{n+1} = q_i^n - \frac{\Delta t}{\Delta x}\left[\left(\sigma^*_{i+\frac{1}{2}}\right)_L - \left(\sigma^*_{i-\frac{1}{2}}\right)_R\right] - (ghS_f)_i^n \Delta t \tag{19}$$

$$\left(\sigma^*_{i+\frac{1}{2}}\right)_L = \sigma^*_{i+\frac{1}{2}} - g\frac{h_{i+1}+h_i}{2}\left(\frac{S_L}{S_R - S_L}\right)_{i+\frac{1}{2}}\left(z_{b,i+1} - z_{b,i}\right)$$

$$\left(\sigma^*_{i-\frac{1}{2}}\right)_R = \sigma^*_{i-\frac{1}{2}} - g\frac{h_{i-1}+h_i}{2}\left(\frac{S_R}{S_R - S_L}\right)_{i+\frac{1}{2}}\left(z_{b,i} - z_{b,i-1}\right)$$

Also integral form sediment continuity equation (Eq. 12) becomes

$$(Z_b)_i^{n+1} = (Z_b)_i^{n+1} - \frac{\Delta t}{\Delta x}\left(\psi^*_{i+\frac{1}{2}} - \psi^*_{i-\frac{1}{2}}\right) \tag{20}$$

For include the influence of the intermediate wave was used HLLC solver.

$$\psi^* = \frac{S^*\psi_L - S_L\psi_R + S^*S_L(Z_{b,R} - Z_{b,L})}{S^* - S_L} \tag{21}$$

2.7 Two-layer model description

A general sketch of a two-layer shallow-water description is given in (Fig. 2) The flow is represented by two moving layers and one layer at rest: (1) a clear-water upper layer, of depth h_w, flowing at an assumed uniform velocity u_w; (2) a moving sediment layer, of depth h_s with a uniform velocity u_s and a volumetric sediment concentration C_s; and (3) a fixed-bed layer extending to the level Z_b, and presenting a concentration C_b. The shallow-water assumption implies a hydrostatic distribution of the pressure in the various layers. At the bed interface Γ_b, erosion or deposition results from an inequality between the entraining shear stress τ_s, exerted by the moving mixture on the bed, and the resisting force τ_b, exerted by the soil against this movement.

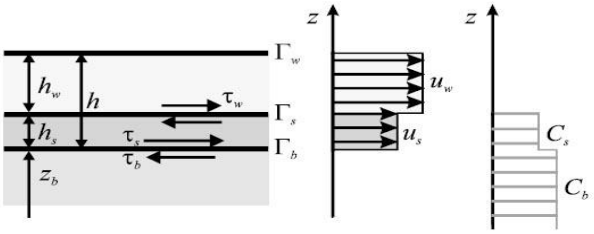

Fig 2: Two-layer description.

In this model, the concentration of sediment Cs in the layer hs is assumed to be equal to C_b and the transport layer hs is assumed to be in movement at the same uniform velocity as the clear-water layer ($u_s = u_w = u$). According to those assumptions the shear stress is supposed to be negligible at the interface Γ_b. Using the above assumptions, the expressions for the continuity of both the sediments and the mixture and for the conservation of flow momentum read.

$$\frac{\partial}{\partial t}(Z_b + h_s) + \frac{\partial}{\partial x}(h_s u) = 0$$

$$\frac{\partial}{\partial t}(Z_b + h_s + h_w) + \frac{\partial}{\partial x}[(h_s + h_w)u] = 0 \tag{22}$$

$$\frac{\partial}{\partial t}\left((h + rh_s)u\right) + \frac{\partial}{\partial x}\left[(h + rh_s)u^2 + \frac{1}{2}gh^2 + \frac{1}{2}rgh_s^2\right] + g(h + rh_s)\frac{\partial Z_b}{\partial x} = -\frac{\tau_s}{\rho_w}$$

$$\frac{\partial Z_b}{\partial t} = -e_b$$

The erosion rate eb, derives from the inequality between the shear stresses acting on both faces of the bed interface

$$e_b = \frac{1}{\rho'_b |u_s|}(\tau_s - \tau_b) \quad , \quad \tau_s = \rho'_s C_f u^2, \quad \tau_b = (\rho'_s - \rho_w) g h_s \tan\phi \tag{23}$$

$$U = \begin{pmatrix} Z_b + h_s \\ Z_b + h_s + h_w \\ h_r u \end{pmatrix}, \; F(U) = \begin{pmatrix} h_s u \\ (h_s + h_w)u \\ h_r u^2 + \frac{1}{2} g(h^2 + r h_s^2) \end{pmatrix} = \begin{pmatrix} q \\ \sigma \\ \psi \end{pmatrix} \tag{24}$$

$$H(U) = \begin{pmatrix} 0 & 0 & 0 \\ 0 & 0 & 0 \\ 0 & 0 & g(h + r h_s) \end{pmatrix} \; , \; S(U) = \begin{pmatrix} 0 \\ 0 \\ -\frac{\tau_s}{\rho_w} \end{pmatrix}$$

fluxes sediment and water continuity was solved by HLL solver simply because there was no source term and flux momentum equation was estimated by HLL and LHLL.

2.8 Boundary and stability condition

For a domain (0,L) discretized into cells I_i , i=1,2,…,m, the conservative formula can be applied to all cells i , i =2,…,m-1. The updating of cells i and m requires the application boundary conditions at x=0, x=L and thus be able to utilize the scheme for i=1, i=m as well. To simulate boundaries

$$h_0^n = h_1^n \quad , \quad u_0^n = u_1^n$$
$$h_{m+1}^n = h_m^n \quad , \quad u_{m+1}^n = u_m^n \tag{25}$$

For stability condition in non-linear systems, such as the shallow water equations

$$\Delta t = \frac{C_{cfl}\Delta x}{S_{max}^n} \quad , \quad S_{max}^n = \max\{|u_i^n| + a_i^n\} \tag{26}$$

Where S_{max}^n is the maximum propagation speed in differential equation. One usually takes $C_{cfl} = 0.9$

3. Results and Analysis

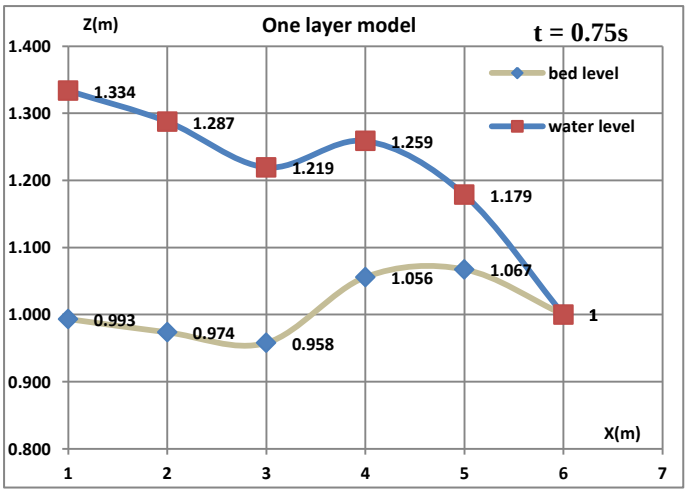

a

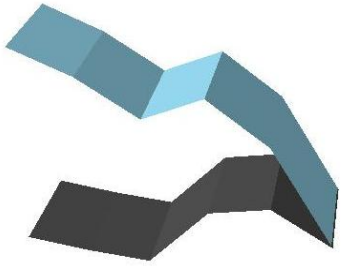

b

Fig 3: One layer model a) dam break after t=0.75 s b) The TIN prepared of dam break

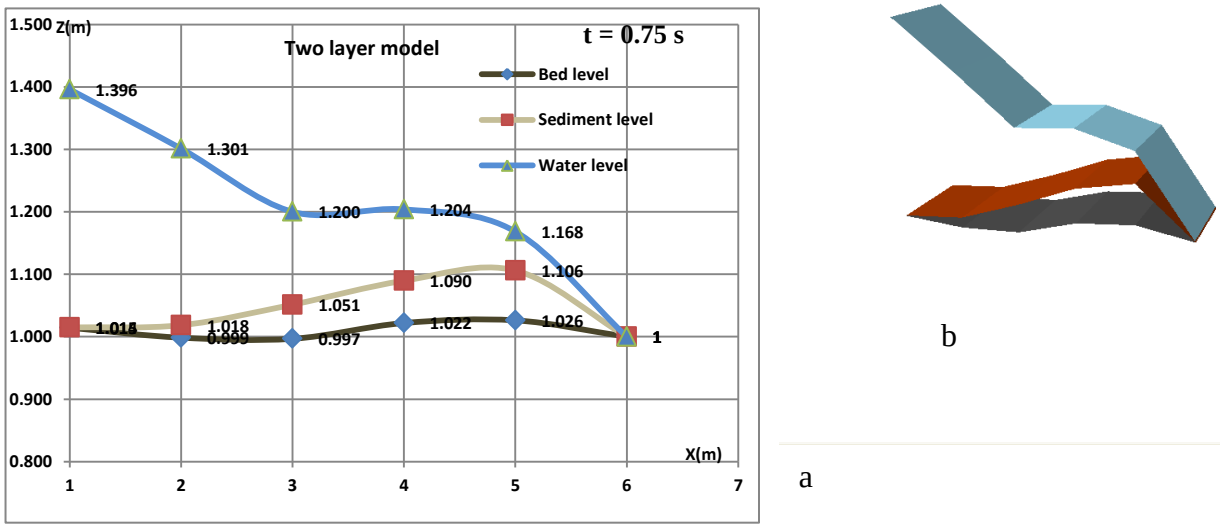

Fig 4: Two layer model a) dam break after t=0.75 s b) The TIN prepared of dam break

condition	volume of water (m^3)	volume of sediment (m^3)
Before dam break	14.93	0
After dam break	22.17	2.2

Table 1. Volume of entrained water and sediment cause of dam break in one layer model by using GIS

Condition	volume(m^3) of water	volume(m^3) of sediment (sediment layer)	volume of (m^3) sediment (bed)	volume of sediment (m^3)
Before dam break	18.9	2.5	0	2.5
After dam break	21.42	5.45	1.05	6.5

Table 2. Volume of entrained water and sediment cause of dam break in two layer model by using GIS

For validating result, experimental and numerical result Zech et al (2008) was used that result had good compatibility by those. Zech et al used C_f =0.04, C_s=0.02, ϕ=20, n=0.026 that in this paper was used the same.

The one-layer model (Fig. 3) is good in representing some features: the front celerity is rather well captured except the trend to spread a little the toe of the water front compared to the rather sharp shape observed. However, overestimated erosion is predicted, which induces a hydraulic jump at the water surface. Regarding the results by the two layer model (Fig. 4), the moving-sediment layer is apparently underestimated, due to the fact that the concentration of this layer is assumed to be the same as the bed material. Sediment transport was shown to be

the outcome of differences in the shear stresses in bed material; the sediment, the bed profile and water surface profile were accurately simulated. In comparison with experimental results, it was shown that larger shear stresses in the bed than that of the sediment, would result in sedimentation and the opposite would result in erosion. To compute the volume of entrained water and sediment, conditions of before dam break and after that were imported into GIS firstly.

By preparing TIN from before dam break and after that, the volumes of water and sediment in this situation have been calculated by Arc map software (Tables 1~2). In one layer model, sediment transport is only due to bed layer (Table 1). While in two layer model, both bed and sediment layer are the causes of sediment transport (Table 2). Volume of sediment entrained of dam break in two layer model almost is two times of one layer model. Besides, the water surface profile is different in two layers model can disaffirm one layer model; not reliable to use for flood mapping

S = Wave speed

Z_b = Bed level

$s = \frac{\rho_s}{\rho_w}$

ρ_s = *Sediment density*

ε_0 = *Porosity*

$\acute{\rho_b}$ = Bottom layer volumetric density

ϕ = Internal friction angle

h = Depth

u = Velocity

U = Variables vector

F = Flux vector

S = Source term vector

a = celerity

$F_{i\mp\frac{1}{2}}$ =numerical flux

5. Conclusions

Sediment transport cause of dame break has been modeled in two modes, namely one-layer and two-layer modeling. In the both models, there is a good agreement among simulation of the wave front, shock waves and discontinuities. GIS facilities provided in the model can be further utilized to develop more consistent flood mapping.

Acknowledgements

Author would like to acknowledge the generous support that he has received from Dr F.Yazdandoost during making this paper.

References

Toro, E.F., (2001), Shock-capturing methods for free-surface shallow flows, john Wiley & sons, Ltd

Zech, Y. and Soares-Frazão, S. and Spinewine, B. and Le Grelle, N., (2008), Dam-break induced sediment movement: Experimental approaches and numerical modeling, journal of hydraulic research, 46 (2), 176–190

George, D.L. (2004), "Numerical Approximation of the Nonlinear Shallow Water Equations with Topography and Dry Beds: A Godunov-Type Scheme," Master of Science thesis, University of Washington.

Castro Dıaz, M.J. and Fernandez-Nieto, E.D. and Ferreiro, A.M., (2008), Sediment transport models in Shallow Water equations and numerical approach by high order finite volume methods , journal of Computers & Fluids, 37, 299-316.

Toro, E.F. and Navarro, P.G., (2007), Godunov-type methods for free-surface shallow flows: A review, journal of hydraulic research, 45 (6), 736–751.